A PDE-ODE model for traffic control with autonomous vehicles

Thibault Liard, Raphael Stern, Maria Laura Delle Monache

A PDE-ODE model for traffic control with autonomous vehicles

Thibault Liard [a], Raphael Stern [b], Maria Laura Delle Monache [c]

[a] *Fundación Deusto, University of Deusto, 48007 Bilbao, Basque Country, Spain*

[b] *Department of Civil, Environmental, and Geo- Engineering, University of Minnesota, Minneapolis, USA*

[c] *Univ. Grenoble Alpes, Inria, CNRS, Grenoble INP, GIPSA-Lab, 38000 Grenoble, France*

Abstract

We introduce a coupled PDE-ODEs model to describe mixed traffic with humans and autonomous vehicles. The partial differential equation describes the bulk of human traffic while the ordinary differential equations characterize the trajectories of possibly many autonomous vehicles. The coupled PDE-ODE model is introduced, and existence of solutions for this model is shown, along with a proposed algorithm to construct approximate solutions. We propose a control strategy for the speeds of the autonomous vehicles to minimize total fuel consumption. Existence of solutions for the optimal control problem is proved, and show numerically that a greater reduction in total fuel consumption is possible with more AVs acting as moving bottlenecks.

Key words: PDE-ODE systems, Traffic control, Autonomous vehicles.

1 Introduction

In recent years, increasing attention has been placed on transportation systems and their management due the increasing number of disrupting technologies developing in this field with potential to alleviate traffic congestion and pollution. One idea that has emerged is the possibility to use a small number of autonomous vehicles in the traffic flow to act as controllers, and control the predominately human-piloted flow of traffic. Despite the many efforts conducted with field experiments (see for example [35]) as well as simulations-based applications [22,11,16,36], a comprehensive macroscopic theory for control of traffic via autonomous vehicles is still missing. Historically, common traffic control strategies involve ramp-metering and variable speed limits (VSL), which have been extensively studied in the literature, see [2,23,17,6,5,8,13,18] and reference therein. In the last decade researchers started studying as well control problems related to scalar or systems of conservation laws with literature coming from control and mathematical communities, see [20,21,34,39,37,38,31,19,3].

More recently, new disruptive technologies such as autonomy and adaptive cruise control (ACC) have paved the road for new types of control. In particular, one can look at Lagrangian control where a certain number of vehicles are controlled within the bulk traffic flow to act as bottlenecks. Recently, two seminal works [29,7] have proposed strategies to control traffic using such an approach. Both these works look to control traffic via means of autonomous vehicles. In particular, [29] uses a model predictive control (MPC) approach to achieve a reduction in fuel consumption in congested traffic due to the presence of a fixed bottleneck on the highway. While in [7], Čicic et al. dissipate traffic jam via the use of controlled autonomous vehicles in a discretized setting using the well-known Cell Transmission Model (CTM) [10].

In this paper, we study a control problem for a coupled Partial Differential Equation-Ordinary Differential Equations (PDE-ODEs) system with application to traffic flow with autonomous vehicles (AVs). This is done by starting from existing models for moving bottlenecks [25,12]. These models are developed from the classical Lighthill-Whitham-Richards (LWR) PDE [28,32] and are augmented with the dynamics of a slower-moving vehicle in the bulk traffic flow that creates a moving bottleneck. The underlying idea behind this paper is to exploit the dynamics of the slower-moving vehicle by controlling it to drive according to a specific control

⋆ This paper was not presented at any IFAC meeting. Corresponding author T. Liard. Tel. +33601857658

Email addresses: thibault.liard@deusto.es (Thibault Liard), rstern@umn.edu (Raphael Stern), ml.dellemonache@inria.fr (Maria Laura Delle Monache).

law. In this way the interaction between the controlled vehicle and the surrounding flow can be used to modify the traffic density to improve congestion and reduce emissions. We consider the speed of the moving bottleneck as the control variable.
The main contribution of the paper is two-fold. First, we extend existing models of moving bottleneck to the problem of multiple moving bottleneck. Then, we analytically prove the existence of solution for the coupled PDE-ODE model and for the optimal control problem. And we show numerically how to solve the optimal control problem.
The paper is organized as follows: Section 2 sets up the problem and shows how to analytically find solutions to the Riemann problem of PDE-ODE systems. In Section 3 we show how to compute approximate solutions to the coupled PDE-ODE system, and in Section 4 we introduce an optimal control problem and prove that this optimal control problem has at least one solution. Section 5 shows the numerical scheme and the simulations.

2 Description of the model

2.1 Coupled PDE-ODE model for traffic with autonomous vehicles

We study a coupled PDE-ODE system modeling the impact of $N \in \mathbb{N}\backslash\{0\}$ autonomous vehicles (AVs) on traffic flow. More precisely, the PDE is the conservation law used in the LWR model [28,32] that describes the evolution of traffic flow:

$$\begin{aligned} &\partial_t \rho\left(t,x\right) + \partial_x f\left(\rho\left(t,x\right)\right) = 0, \quad t>0,\, x \in \mathbb{R}, \\ &\rho(0,x) = \rho_0(x), \quad x \in \mathbb{R}. \end{aligned} \tag{1}$$

Let $\rho_{\max}$ and $V_{\max}$ be respectively the constant maximal density and the constant maximal speed of a road. Then above, $\rho = \rho(t,x) \in [0, \rho_{\max}]$ denotes the macroscopic traffic density for every time $t \geq 0$ and position $x \in \mathbb{R}$. The flux function f is defined such that $f(\rho) = \rho v(\rho)$ with v the mean speed of cars. In this case, we assume that the speed v depends linearly on the density of cars as follows:

$$v(\rho) = V_{\max}\left(1 - \frac{\rho}{\rho_{\max}}\right).$$

For $i \in \{1, \cdots, N\}$, the trajectory of the i^{th} autonomous vehicle is modeled by the following ODE

$$\begin{aligned} &\dot{y}_i(t) = \min\{V_i(t), v(\rho(t, y_i(t)+))\}, \quad t>0, \\ &y_i(0) = y_i^0. \end{aligned} \tag{2}$$

Above, $v(\rho(t,y_i(t)+)) := \lim\limits_{\substack{x \to y_i(t) \\ x > y_i(t)}} \rho(t,x)$, which indicates that the autonomous vehicle is affected only by the density downstream. The i^{th} AV drives at its maximum desired speed V_i except when the traffic in front is too dense. In that case, the autonomous vehicle has to reduce its velocity accordingly.
To describe the influence of the i^{th} AV on the evolution of traffic we introduce the following flux constraint:

$$f\left(\rho\left(t, y_i(t)\right)\right) - \dot{y}_i(t)\rho\left(t, y_i(t)\right) \leq F_\alpha\left(\dot{y}_i(t)\right), \quad t>0. \tag{3}$$

Where the term F_α, that indicates the maximal flux allowed in the i^{th} autonomous vehicle reference frame, is defined as follows:

$$F_\alpha(\dot{y}_i(t)) := \alpha \max_{\rho \in [0, \rho_{\max}]} \left(f(\rho) - \dot{y}_i(t)\rho\right).$$

In particular, the road capacity is reduced by a factor $\alpha \in (0,1)$ due to the presence of the AVs. The complete model then becomes:

$$\begin{cases} \partial_t \rho\left(t,x\right) + \partial_x f\left(\rho\left(t,x\right)\right) = 0 \\ \dot{y}_i(t) = \min\{V_i(t), v(\rho(t, y_i(t)+))\} \\ f\left(\rho\left(t, y_i(t)\right)\right) - \dot{y}_i(t)\rho\left(t, y_i(t)\right) \leq F_\alpha\left(\dot{y}_i(t)\right) \\ \rho(0,x) = \rho_0(x) \\ y_i(0) = y_i^0 \end{cases} \tag{4}$$

A similar coupled PDE-ODE system (4) was introduced in [12] for a single AV and a constant maximum speed. For simplicity of notation, in the rest of this section we drop the index i and denote $V_i = V$.
Let us fix $\check{\rho}_\alpha(V)$ and $\hat{\rho}_\alpha(V)$ the two density values solutions of $F_\alpha(V) + V\rho = f(\rho)$ such that $\check{\rho}_\alpha(V) < \hat{\rho}_\alpha(V)$. And let ρ^* the solution of $V\rho = f(\rho)$ (see Figure 1). We compute $\check{\rho}_\alpha(V)$, $\hat{\rho}_\alpha(V)$ and ρ^* using the fact that f is strictly concave and $v(\rho) = V_{\max}\left(1 - \frac{\rho}{\rho_{\max}}\right)$. For every $V \in [0, V_{\max}]$, we obtain:

$$\check{\rho}_\alpha(V) = \rho_{\max}(V_{\max} - V)\left(\frac{1 - \sqrt{1-\alpha}}{2V_{\max}}\right), \tag{5}$$

$$\hat{\rho}_\alpha(V) = \rho_{\max}(V_{\max} - V)\left(\frac{1 + \sqrt{1-\alpha}}{2V_{\max}}\right), \tag{6}$$

$$\rho^*(V) = \rho_{\max}\left(1 - \frac{V}{V_{\max}}\right). \tag{7}$$

Moreover, we denote by $\sigma(\rho_1, \rho_2) := \frac{f(\rho_1) - f(\rho_2)}{\rho_1 - \rho_2}$ the Rankine-Hugoniot speed of the front wave (ρ_1, ρ_2).

2.2 The Riemann problem with moving constraints

Let us recall how to construct the solution of a Riemann problem for a constrained system. Consider the coupled PDE-ODE (1)-(2)-(3) system equipped with Riemann

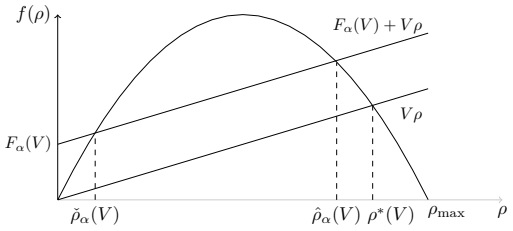

Fig. 1. The flux function f and $\check{\rho}_\alpha(V) \leqslant \hat{\rho}_\alpha(V) \leqslant \rho^*(V)$.

type initial data

$$\rho_0(x) = \begin{cases} \rho_L \text{ if } & x < 0 \\ \rho_R \text{ if } & x > 0 \end{cases} \quad \text{and} \quad y_0 = 0. \tag{8}$$

Following [12, Section 3] and [15], we denote by $\mathcal{R}$ the standard Riemann solver for the simple PDE (1) with ρ_0 as in (8) and we denote by $\mathcal{R}^V$ the constrained Riemann problem.

Definition 1. *Let $V \in [0, V_{\max}]$. The constrained Riemann solver $\mathcal{R}^V : [0,\rho_{\max}]^2 \mapsto L^1_{loc}(\mathbb{R}; [0,\rho_{\max}])$ for (1)-(2)-(3) and (8) is defined as follows:*

(1) If $f(\mathcal{R}(\rho_L,\rho_R)(V)) > F_\alpha(V) + V\mathcal{R}(\rho_L,\rho_R)(V)$, then

$$\mathcal{R}^V(\rho_L,\rho_R)(x/t) = \begin{cases} \mathcal{R}(\rho_L, \hat{\rho}_\alpha(V))(x/t) \ \text{if} & x < Vt, \\ \mathcal{R}(\check{\rho}_\alpha(V), \rho_R)(x/t) \ \text{if} & x \geqslant Vt, \end{cases}$$

and $y(t) = Vt$.

(2) If $V\mathcal{R}(\rho_L,\rho_R)(V) \leqslant f(\mathcal{R}(\rho_L,\rho_R)(V)) \leqslant F_\alpha(V) + V\mathcal{R}(\rho_L,\rho_R)(V)$, then

$$\mathcal{R}^V(\rho_L,\rho_R) = \mathcal{R}(\rho_L,\rho_R) \quad \text{and} \quad y(t) = Vt.$$

(3) If $f(\mathcal{R}(\rho_L,\rho_R)(V)) < V\mathcal{R}(\rho_L,\rho_R)(V)$, then

$$\mathcal{R}^V(\rho_L,\rho_R) = \mathcal{R}(\rho_L,\rho_R) \quad \text{and} \quad y(t) = v(\rho_R)t.$$

An illustration of each case in Definition 1 is given in Figure 2a, Figure 2b and Figure 2c. In particular, in Figure 2a, a shock $(\hat{\rho}_\alpha, \check{\rho}_\alpha)$ which doesn't satisfy the Lax entropy condition [24] is shown. Such a shock is called *a non-classical shock*.

3 Wave-front tracking algorithm

In this section, we describe how to construct solutions to the coupled PDE-ODE system. Let the initial density ρ_0 and the initial trajectories of the autonomous vehicle $(y_i^0)_{i\in\{1,\cdots,N\}}$ be known. Following [15], we can construct a density mesh $\mathcal{M}_n$ on the interval $[0,\rho_{\max}]$ and a velocity mesh $\mathcal{V}_n$ on the interval $[0, V_{\max}]$ such that $(\check{\rho}_\alpha(V_i), \hat{\rho}_\alpha(V_i)) \in (\mathcal{M}_n)^2$ for every $i \in \{1,\cdots,N\}$ and for every $V_i \in \mathcal{V}_n$. Simultaneously, for every $i \in \{1,\cdots,N\}$, we consider a sequence of piecewise constant functions $(V_i^n)_{n\in\mathbb{N}}$ and a sequence $(\rho_0^n)_{n\in\mathbb{N}}$ having both a finite number of discontinuities such that

$$\lim_{n\to+\infty} \|\rho_0^n - \rho_0\|_{L^1(\mathbb{R})} = 0 \quad \text{and} \quad TV(\rho_0^n) \leqslant TV(\rho_0), \tag{9}$$

$$\lim_{n\to+\infty} \|V_i^n - V_i\|_{L^1(\mathbb{R}^+)} = 0 \quad \text{and} \quad TV(V_i^n) \leqslant TV(V_i). \tag{10}$$

We adapt the method in [9] to construct approximate wave-front tracking solutions.

Remark 1. *Hereafter, the term "approximately" means that a rarefaction wave is split into a fan of rarefaction shocks such that the left and the right densities of each rarefaction shock belongs to the state mesh $\mathcal{M}_n$.*

Step 1 For every $i \in \{1,\cdots,N\}$, we solve approximately the constrained Riemann problem at $x = y_i^0$ as described in Section 2.2. This is done for $t \in [0, t_1^n]$ with $V = V_i(0+)$ where t_1^n is the first time when one of the AVs changes its speed.

Step 2 At each point of discontinuity of ρ_0^n different from $(y_i^0)_{i=1,\cdots,N}$, we solve approximately the standard Riemann problem over $[0, t_1^n]$.

Step 3 By piecing solutions together, we construct a solution ρ^n and for every $i \in \{1,\cdots,N\}$, y_i^n is solution of

$$\begin{cases} \dot{y}_i^n(t) = \min(V_i^n(t), v(\rho^n(t, y_i^n(t)+))), \\ y_i^n(0) = y_i^0, \end{cases}$$

until two waves meet at t_I.

Step 4 Now we check the value of t_I:

(a) If $t_I < t_1^n$, then the approximate solution $\rho^n(t_I,\cdot)$ is still a piecewise constant function verifying $\rho^n(t_I, x) \in \mathcal{M}_n$ for almost every $x \in \mathbb{R}$. Thus, **Step 1**, **Step 2** and **Step 3** are repeated until two waves meet at a new t_I until $t_I \geqslant t_1^n$.

(b) If $t_I = t_1^n$, the constrained Riemann problem is solved over $[t_1^n, t_2^n]$ as previously replacing $V_i(0+)$ by $V_i(t_1^n+)$ for every $i \in \{1,\cdots,N\}$ where t_2^n is the second time when one of the AVs changes its speed.

Using this approach, we construct an approximate solution $(\rho^n, y_1^n, \cdots, y_N^n)$ of (1)-(2)-(3).

4 Control problem

4.1 The Cauchy problem

We denote with BV the set of functions of bounded variation endowed with the norm $\|u\|_{BV} = \|u\|_{L^1} + TV(u)$

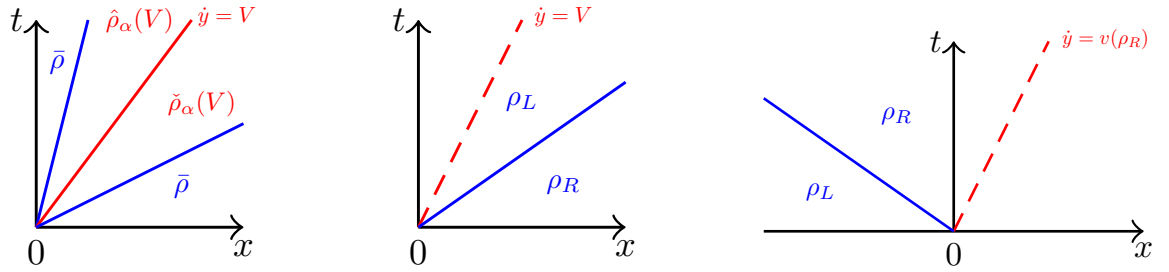

(a) Case (1) of Definition 1: $\rho_L = \rho_R = \bar\rho \in (\check\rho_\alpha(V), \hat\rho_\alpha(V))$.

(b) Case (2) of Definition 1: $0 < \rho_L < \check\rho_\alpha(V)$ and $\hat\rho_\alpha(V) < \rho_R \leqslant \rho_{\max}$.

(c) Case (3) of Definition 1: $\rho^*(V) < \rho_L < \rho_R$.

Fig. 2. Possible different solutions of the Riemann problem

where $TV(u)$ stands for the total variation of u, see [14]. Let us consider a sequence of initial positions $(y_i^0)_{i=1,\cdots,N} \in \mathbb{R}^N$, a sequence of maximum speeds $(V_i)_{i=1,\cdots,N} \in BV\left(\mathbb{R}^+;[0,V_{\max}]\right)^N$ and a initial density $\rho_0 \in \left(L^1 \cap BV\right)(\mathbb{R};[0,\rho_{\max}])$.

Definition 2. *The $(n+1)$-tuple $(\rho, y_1, \cdots, y_N)$ provides a solution to (1)-(2)-(3) if the following conditions hold.*

(1) $\rho \in C^0\left(\mathbb{R}^+;\left(L^1 \cap BV\right)(\mathbb{R};[0,\rho_{\max}])\right)$;
(2) For every $i \in \{1,\cdots,N\}$, $y_i \in W^{1,1}_{loc}(\mathbb{R}^+;\mathbb{R})$; .
(3) ρ *is a weak solution of* $\partial_t\rho + \partial_x f(\rho) = 0$, $(x,t) \in \mathbb{R}^+ \times \mathbb{R}$;
(4) For every $\kappa \in \mathbb{R}$, *for all* $\varphi \in C^1_c(\mathbb{R}^2;\mathbb{R}^+)$ *and for every* $i \in \{1,\cdots,N\}$, *it holds*

$$\int_{\mathbb{R}^+}\int_{\mathbb{R}} \left(|\rho-\kappa|\partial_t\varphi + sgn(\rho-\kappa)g(k)\partial_x\varphi\right) dx\, dt \tag{11}$$

$$+2\int_{\mathbb{R}^+} \left(h_i(k) - \min\{h_i(k), F_\alpha(\dot y_i(t))\}\right)\varphi(t,y_i(t))\, dt \tag{12}$$

$$+\int_{\mathbb{R}} |\rho_0-\kappa|\varphi(0,x)\, dx \geqslant 0\,;$$

with $g(k) = f(\rho) - f(\kappa)$ *and* $h_i(k) = f(\kappa) - \dot y_i(t)\kappa$.
(5) For a.e. $t > 0$, *for every* $i \in \{1,\cdots,N\}$, $\dot y_i(t) = \min\left(V_i(t), v\left(\rho\left(t,y_i(t)+\right)\right)\right)$;
(6) For a.e. $t > 0$, *for every* $i \in \{1,\cdots,N\}$ $f\left(\rho\left(t,y_i(t)\pm\right)\right) - \dot y_i(t)\rho\left(t,y_i(t)\pm\right) \leq F_\alpha\left(\dot y_i(t)\right)$;

The Cauchy problem of (1)-(2)-(3) has been already studied in [12,26,27,15] when only one autonomous vehicle ($N = 1$ in (2) and (3)) influences the traffic flow. When the maximum speed of the AV is constant in time, the existence and the stability of solutions for (1)-(2)-(3) in the sense of Definition 2 has been proven in [12,26,27]. When the maximum speed of the AV depends on time, the authors in [15] proved the existence of solutions for (1)-(2)-(3). Here we introduce several AVs.

Let $\epsilon > 0$. We introduce the class of admissible maximum speed $\mathcal{V}_N^\epsilon \subset BV\left(\mathbb{R}^+;[0,V_{\max}]\right)^N$ as follows. The sequence $(V_i)_{i\in\{1,\cdots,N\}} \in \mathcal{V}_N^\epsilon$ if, for every $t \geqslant 0$, for every $i \in \{1,\cdots,N-1\}$,

$$y_i(t) - \epsilon < y_{i+1}(t),$$

where y_i is solution of (2). Note that the set $\mathcal{V}_N^\epsilon$ depends on the initial density ρ_0 and the initial position of the N autonomous vehicles $(y_i^0)_{i\in\{0,\cdots,N\}}$. When $(V_i)_{i\in\{1,\cdots,N\}} \in \mathcal{V}_N^\epsilon$, an autonomous vehicle can never catch up the autonomous vehicle in front. Mathematically speaking, two non-classical shocks cannot interact.

Theorem 1. *Let $\epsilon > 0$, $N \in \mathbb{N}\backslash\{0\}$, $\rho_0 \in BV(\mathbb{R},[0,\rho_{\max}])$ and $(y_i^0)_{i=1,\cdots,N} \in \mathbb{R}^N$. We assume that $(V_i)_{i\in\{1,\cdots,N\}} \in \mathcal{V}_N^\epsilon$. The Cauchy problem (1)-(2)-(3) admits a solution in the sense of Definition 2.*

Proof. We contruct piecewise constant approximate solutions (ρ^n, y^n) of (1)-(2)-(3) via the wave-front tracking method described in Section 3. Then, we introduce the following TV type functional $\Gamma(t)$ defined by

$$\begin{aligned}\Gamma(t) &= TV\left(\rho^n(t,\cdot)\right) + 2\rho_{\max} + \textstyle\sum_{i=1}^N \gamma_i(t) \\ &\quad + \tfrac{3\rho_{\max}}{V_{\max}} \textstyle\sum_{i=1}^N TV\left(V_i^n(\cdot);[t,+\infty[\right),\end{aligned} \tag{13}$$

where if $\rho^n(t,y_i^n(t)-) = \hat\rho_\alpha(V_i^n(t))$ and $\rho^n(t,y_i^n(t)+) = \check\rho_\alpha(V_i^n(t))$ then $\gamma_i(t) = -2\left(\hat\rho_\alpha(V_i^n(t)) - \check\rho_\alpha(V_i^n(t))\right)$, otherwise $\gamma_i(t) = 0$. Roughly, γ_i is a function created to compensate the possible interactions between the wave-fronts and the i^{th} autonomous vehicle. It is clear that Γ is well-defined for a.e $t \geqslant 0$ and it changes only at discontinuity points of V_i^n with $i \in \{1,\cdots,N\}$ or when two wave-fronts interacts.

- Assuming that an interaction occurs at time $t = \bar{t}$ away from $(y_i(\bar{t}))_{i\in\{1,\cdots,N\}}$. In this case, either two shocks collide or a shock and a rarefaction shock interact. In both cases, we have $TV(\rho^n(\bar{t}+,\cdot)) \leqslant TV(\rho^n(\bar{t}-,\cdot))$ and, for every $i \in \{1,\cdots,N\}$, $\gamma_i(\bar{t}+) = \gamma_i(\bar{t}-)$ and $TV\left(V_i^n(\cdot);[\bar{t}+,+\infty[\right) = TV\left(V_i^n(\cdot);[\bar{t}-,+\infty[\right)$ leading to $\Gamma(\bar{t}+) \leqslant \Gamma(\bar{t}-)$.
- Since $(V_i)_{i\in\{1,\cdots,N\}} \in \mathcal{V}_N^\epsilon$, all possible interactions between classical waves (shocks and rarefaction shocks) and the i^{th} autonomous vehicle are described in [12,26]. In that case, for every $i \in \{1,\cdots,N\}$, $V_i^n(\bar{t}-) = V_i^n(\bar{t}+)$. From [26, Lemma 2], $TV\left(\rho^n(\bar{t}+,\cdot)\right) + 2\rho_{\max} + \sum_{i=1}^N \gamma_i(\bar{t}+) \leqslant TV\left(\rho^n(\bar{t}-,\cdot)\right) + 2\rho_{\max} + \sum_{i=1}^N \gamma_i(\bar{t}-)$. Therefore, $\Gamma(\bar{t}+) \leqslant \Gamma(\bar{t}-)$.
- Using $(V_i)_{i\in\{1,\cdots,N\}} \in \mathcal{V}_N^\epsilon$, all possible situations when a jump occur in V_i^n are described in [15]. From [15, Lemma 3.1,Lemma 3.2,Lemma 3.3], $\Gamma(\bar{t}+) \leqslant \Gamma(\bar{t}-)$.

We conclude that

$$\Gamma(\bar{t}+) \leqslant \Gamma(\bar{t}-). \tag{14}$$

From (9), (10) and (14),

$$TV(\rho^n(t,\cdot)) \leqslant TV(\rho_0) + 2N\rho_{\max} + \frac{3\rho_{\max}}{V_{\max}} \sum_{i=1}^N TV(V_i). \tag{15}$$

Since $(V_i)_{i\in\{1,\cdots,N\}} \in \mathcal{V}_N^\epsilon$ and there exists $C > 0$ such that $TV(\rho^n(t,\cdot)) \leqslant C$, we can apply [15, Lemma 3.4]. Thus, up to a subsequence, we have

$$\rho^n \to \rho, \qquad \text{in } L^1_{\text{loc}}(\mathbb{R}^+ \times \mathbb{R}; [0,\rho_{\max}]), \tag{16a}$$

$$y^n \to y, \qquad \text{in } L^\infty_{\text{loc}}(\mathbb{R}^+; \mathbb{R}), \tag{16b}$$

$$\dot{y}^n \to \dot{y}, \qquad \text{in } L^1_{\text{loc}}(\mathbb{R}^+; \mathbb{R}), \tag{16c}$$

with $TV(\rho(t,\cdot)) \leqslant \liminf_n TV(\rho^n(t,\cdot)) \leqslant C$. In [15, Proof of Theorem 3.1], the author show that the limit (ρ, y) is a solution of (1)-(2)-(3) in the sense of Definition 2. This can be applied since $(V_i)_{i\in\{1,\cdots,N\}} \in \mathcal{V}_N^\epsilon$. More precisely, all possible interactions between waves (shock, rarefaction wave, AVs) are the same as the ones in [15]. □

4.2 The optimal control problem

The objective of the optimization is to drive the AV in such a way that it minimizes the fuel consumption of the entire traffic flow, i.e. the total fuel consumption of all vehicles. Therefore, the control functions are the maximum speed of AVs, denoted by $V_1,\cdots,V_N$.

It is important to be able to quantify the fuel consumption as a function of the vehicle density, which can be integrated over the entire roadway to calculate the total fuel consumed. Fuel consumption is related to the speed of vehicles as shown by [1] and [4]. Generally, fuel consumption increases with the speed of the vehicle, with a nonlinear relationship between speed and fuel consumption. Using the fuel consumption rates of four different commercially available vehicles, [30] obtained the following best-fit model for fuel rate $K(v)$ in liters per hour (ℓ/h) as a function of speed v:

$$\begin{aligned} K(v) = 5.7\times10^{-12}v^6 - 3.6\times10^{-9}v^5 + 7.6\times10^{-7}v^4 \\ -6.1\times10^{-5}v^3 + 1.9\times10^{-3}v^2 + 1.6\times10^{-2}v + 0.99 \end{aligned}$$

for speed v in km/h and fuel consumption rate K in units of ℓ/h. This relationship is depicted in Figure 3a. Using the relationship between speed and fuel rate in Figure 3a as well as the relationship between density and speed in (2.1) obtained by assuming the LWR model, it is possible to compute the fuel rate $F(\rho)$ as a function of traffic density with units ℓ/h by computing:

$$F(\rho) = \rho K(v(\rho)), \tag{17}$$

which is depicted in Figure 3b.

Let $\epsilon > 0$, $T_f > 0$, $C > 0$ and $x_1, x_2 \in \mathbb{R}$ such that $x_1 < x_2$. Fix $\rho_0 \in \left(L^1 \cap BV\right)(\mathbb{R}; [0,\rho_{\max}])$ and for every $i \in \{1,\cdots,N\}$, $y_i^0 \in \mathbb{R}$. We consider thus the following optimal problem

$$\inf_{\substack{(V_i)_{i=1,\cdots,N}\in\mathcal{V}_N^\epsilon \\ \|V_i\|_{BV}\leqslant C}} \mathbf{TFC}(V) := \int_0^{T_f}\int_{x_1}^{x_2} F(\rho(t,x))dtdx, \tag{18}$$

where $V = (V_1,\cdots,V_N)$, the set $\mathcal{V}_N^\epsilon$ is defined in Section 4.1 and (ρ, y) is the solution of (1)-(2)-(3) associated to (ρ_0, y_0). The functional **TFC** represents the Total Fuel Consumption computed on a highway section of length $x_2 - x_1$ km during T_f hours.

Theorem 2. *The optimal problem* (18) *has at least one optimal solution.*

Proof. There exists a minimizing sequence $(V^m)_{m\in\mathbb{N}}$ verifying that

$$\inf_V \mathbf{TFC}(V) \leqslant \mathbf{TFC}(V^m) \leqslant \inf_V \mathbf{TFC}(V) + \frac{1}{m}.$$

with $V^m = (V_i^m)_{i=1,\cdots,N} \in \mathcal{V}_N^\epsilon$ and for every $i \in \{1,\cdots,N\}$, $\|V_i^m\|_{BV} \leqslant C$.

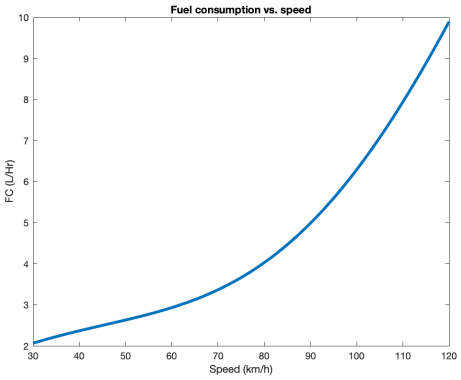

(a) Fuel consumption of a vehicle as a function of vehicle speed.

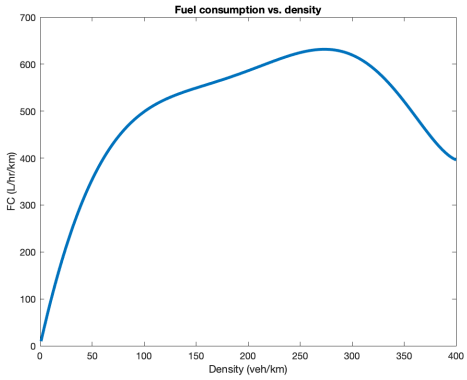

(b) Fuel consumption rate of the bulk traffic flow as a function of traffic density

Fig. 3. Fuel consumption vs.speed and density according to [30]

Fix $m \in \mathbb{N}$. Since $\rho_0 \in BV(\mathbb{R};[0,\rho_{\max}])$ and $V_i^m \in BV([0,T_f];[0,V_{\max}])$, there exists an approximate density ρ_0^n of ρ_0 and an approximate maximum speed $V_i^{m,n}$ of V_i^m such that

$$\lim_{n\to+\infty} \|\rho_0^n - \rho_0\|_{L^1(\mathbb{R})} = 0 \text{ and } TV(\rho_0^n) \leqslant TV(\rho_0), \tag{19}$$

$$\begin{aligned} \lim_{n\to+\infty} \|V_i^{m,n} - V_i^m\|_{L^1(\mathbb{R}^+)} &= 0 \\ \text{and } TV(V_i^{m,n}) &\leqslant TV(V_i^m). \end{aligned} \tag{20}$$

for every $i \in \{1,\cdots,N\}$. As in the proof of Theorem 1, we construct an approximate solution $(\rho^{m,n}, y_1^{m,n},\cdots,y_N^{m,n})$ of (1)-(2)-(3) such that

$$TV(\rho^{m,n}(t,\cdot)) \leqslant TV(\rho_0) + 2N\rho_{\max} + \frac{3\rho_{\max}}{V_{\max}} \sum_{i=1}^{N} TV(V_i^m). \tag{21}$$

Then, up to a subsequence, $(\rho^{m,n}, y_1^{m,n},\cdots,y_N^{m,n})$ converges to a solution $(\rho^m, y_1^m,\cdots,y_N^m)$ of (1)-(2)-(3) with $V = V^m$ as $n \to \infty$ and

$$TV(\rho^m(t,\cdot)) \leqslant \liminf_n TV(\rho^{m,n}(t,\cdot)). \tag{22}$$

In particular, we have

$$\lim_{n\to\infty} \|\rho^{m,n}(t,\cdot) - \rho^m(t,\cdot)\|_{L^1([x_1,x_2];[0,\rho_{\max}])} = 0.$$

Moreover, using (21), (22) and $\|V_i^m\|_{BV} \leqslant C$, there exists a positive constant, still denoted by $C > 0$, independent of n and m such that

$$\max(TV(\rho^m), TV(\rho^{m,n})) \leqslant C.$$

By dominated convergence theorem,

$$\lim_{n\to\infty} \int_0^{T_f}\int_{x_1}^{x_2} F(\rho^{m,n})dtdx = \int_0^{T_f}\int_{x_1}^{x_2} F(\rho^m)dtdx. \tag{23}$$

Using that V^m is a minimizing sequence and (20), we deduce that, for every $i \in \{1,\cdots,N\}$,

$$\|V_i^{m,n}\|_{BV} \leqslant C + \frac{1}{n}, \tag{24}$$

and

$$y_i^{m,n}(t) - \epsilon + \frac{1}{n} \leqslant y_{i+1}^{m,n}(t). \tag{25}$$

From (23), there exists a function $\varphi : m \to \mathbb{N}$ strictly increasing such that

$$|\mathbf{TFC}(V_{m,\varphi(m)}) - \mathbf{TFC}(V_m)| \leqslant \frac{1}{m}. \tag{26}$$

Using (24), we have

$$\|V_i^{m,\varphi(m)}\|_{BV} \leqslant C + \frac{1}{\varphi(m)}, \tag{27}$$

Note that $(V^{m,\varphi(m)})_{m\in\mathbb{N}}$ is not a minimizing sequence. Helly's Theorem, see [33, Theorem 7.25], implies that there exists a function $\bar{V} \in BV([0,T_f];[0,V_{\max}])^N$ and a subsequence of $V^{m,\varphi(m)}$, still denoted by $V^{m,\varphi(m)}$, such that $V_i^{m,\varphi(m)}$ converges to $\bar{V}_i$ in $L^1([0,T_f];[0,V_{\max}])$ and $TV(\bar{V}_i) \leqslant \liminf_m TV(V_i^{m,\varphi(m)}) \leqslant C$. From (27), we

have

$$\begin{aligned}\|\bar{V}_i\|_{BV} &\leqslant \|\bar{V}_i - V_i^{m,\varphi(m)}\|_{L^1} + \|V_i^{m,\varphi(m)}\|_{L^1} + TV(\bar{V}_i),\\ &\leqslant \|\bar{V}_i - V_i^{m,\varphi(m)}\|_{L^1} + \|V_i^{m,\varphi(m)}\|_{L^1}\\ &\qquad + \liminf_m TV(V_i^{m,\varphi(m)}),\\ &= \liminf_m \|V_i^{m,\varphi(m)}\|_{L^1} + \liminf_m TV(V_i^{m,\varphi(m)}),\\ &\leqslant \liminf_m \|V_i^{m,\varphi(m)}\|_{BV} \leqslant C.\end{aligned} \tag{28}$$

Note that $(\rho^{m,\varphi(m)}, y_1^{m,\varphi(m)}, \cdots, y_N^{m,\varphi(m)})$ is an approximate solution of (1)-(2)-(3) with $V = \bar{V}$. As in the proof of Theorem 1, we have

$$TV(\rho^{m,\varphi(m)}(t,\cdot)) \leqslant TV(\rho_0) + 2N\rho_{\max} + \frac{3\rho_{\max}}{V_{\max}} \sum_{i=1}^{N} TV(\bar{V}_i). \tag{29}$$

Then, up to a subsequence, $(\rho^{m,\varphi(m)}, y_1^{m,\varphi(m)}, \cdots, y_N^{m,\varphi(m)})$ converges to a solution $(\rho, y_1, \cdots, y_N)$ of (1)-(2)-(3) with $V = \bar{V}$ as $m \to \infty$ and

$$TV(\rho(t,\cdot)) \leqslant \liminf_m TV(\rho^{m,\varphi(m)}(t,\cdot)). \tag{30}$$

In particular, we have

$$\lim_{m\to\infty} \|\rho^{m,\varphi(m)}(t,\cdot) - \rho(t,\cdot)\|_{L^1([x_1,x_2];[0,\rho_{\max}])} = 0.$$

and for every $i \in \{1, \cdots, N\}$

$$\lim_{m\to\infty} \|y_i^{m,\varphi(m)} - y_i\|_{L^\infty([0,T];\mathbb{R})} = 0. \tag{31}$$

Moreover, using (29), (30) and $TV(\bar{V}_i) \leqslant C$, there exists a positive constant, still denoted by $C > 0$, independent of m such that

$$TV(\rho) \leqslant TV(\rho^{m,\varphi(m)}) \leqslant C.$$

By dominated convergence theorem,

$$\lim_{m\to\infty} \int_0^{T_f}\int_{x_1}^{x_2} F(\rho^{m,\varphi(m)})dtdx = \int_0^{T_f}\int_{x_1}^{x_2} F(\rho)dtdx, \tag{32}$$

where $(\rho, y_1, \cdots, y_N)$ is a solution of (1)-(2)-(3) with $V = \bar{V}$. Using that V^m is a minimizing sequence, (26) and (32), we deduce that

$$\int_0^{T_f}\int_{x_1}^{x_2} F(\rho)dtdx = \inf_V \mathbf{TFC}(V). \tag{33}$$

From (31) and (25) with $n = \varphi(m)$, for every $i \in \{1, \cdots, N\}$, we have

$$y_i(t) - \epsilon \leqslant y_{i+1}(t). \tag{34}$$

Combining (28), (33) and (34), we conclude that $\bar{V}$ is an optimal solution of (18). □

Lemma 1. *The cost function **TFC** is not differentiable with respect to V*

Proof. To prove Lemma 1, it is enough to exhibit an example. Let $V_{\max} = 1$, $\rho_{\max} = 1$, $V \in [0, V_{\max}]$ and one autonomous vehicle drives on the road ($N = 1$), we assume that, for every $x \in \mathbb{R}$, $\rho_0(x) = \check{\rho}_\alpha(V)$ where $\check{\rho}_\alpha(V)$ is defined in (5) and $y_0 = 0$. Then the solution ρ of (1)-(2)-(3) associated to V, ρ_0 and y_0 is, for every $(t,x) \in [0,T] \times [x_1, x_2]$,

$$\rho(t,x) = \check{\rho}_\alpha(V) \text{ and } y(t) = Vt. \tag{35}$$

Let $\epsilon > 0$ and we denote by ρ_ϵ the solution of (1)-(2)-(3) associated to $V + \epsilon$, ρ_0 and y_0. In this case, we have $\check{\rho}_\alpha(V+\epsilon) < \check{\rho}_\alpha(V) < \hat{\rho}_\alpha(V+\epsilon) < \hat{\rho}_\alpha(V)$. Thus the flux constraint is active and so a non-classical shock $(\hat{\rho}_\alpha(V+\epsilon), \check{\rho}_\alpha(V+\epsilon))$ is created. We deduce that, for every $t \in [0,T]$, for every $x \in [x_1, x_2]$, $\rho^\epsilon(t,x) =$

$$\begin{cases} \check{\rho}_\alpha(V), & \text{if } x < (V + \epsilon C_\alpha^+)t\\ \hat{\rho}_\alpha(V) - \epsilon C_\alpha^+, & \text{if } (V + \epsilon C_\alpha^+)t < x < (V+\epsilon)t\\ \check{\rho}_\alpha(V) - \epsilon C_\alpha^-, & \text{if } (V+\epsilon)t < x < (f'(\check{\rho}_\alpha(V)) + \epsilon C_\alpha^-)t\\ \check{\rho}_\alpha(V), & \text{if } (f'(\check{\rho}_\alpha(V)) + \epsilon C_\alpha^-)t < x, \end{cases} \tag{36}$$

with $C_\alpha^- = \frac{1-\sqrt{1-\alpha}}{2V_{\max}}$ and $C_\alpha^+ = \frac{1+\sqrt{1-\alpha}}{2V_{\max}}$. Using (35) and (36), we conclude that the expression

$$\lim_{\epsilon\to 0} \frac{\rho^\epsilon(t,\cdot) - \rho(t,\cdot)}{\epsilon} \tag{37}$$

does not define any L^p-function. Note that (37) can be interpreted as a weak limit in a space of measures:

$$\begin{aligned}\tfrac{\rho^\epsilon(t,\cdot)-\rho(t,\cdot)}{\epsilon} \rightharpoonup\ & (1 - C_\alpha^+)t(\hat{\rho}_\alpha(V) - \check{\rho}_\alpha(V))\delta_{y(t)}(\cdot)\\ & -C_\alpha^- \mathbb{1}_{(y(t), f'(\check{\rho}_\alpha(V))t)}(\cdot)\end{aligned}$$

with $\delta_{y(t)}(\cdot)$ the Dirac measure. □

Remark 2. *Note that the optimal problem* (18) *may admit multiple solutions. For instance, if the initial datum $\rho_0 = \rho_{\max}$ and $N = 1$, then $V \to \mathbf{TFC}(V)$ is a constant function. Therefore, any $V \in BV([0,T_f],[0,V_{\max}])$ such that $\|V\|_{BV} \leqslant C$ is an optimal solution of* (18).

Remark 3. *A gradient descent algorithm to solve the optimal problem* (18) *cannot be applied in a general way.*

5 Simulation results

In this section, we present a numerical example to demonstrate how AVs can be used as moving bottlenecks to control the flow of traffic and optimize the fuel

consumption of the overall traffic flow. The specific scenario considered in this numerical example is explained, as well as the numerical strategy for optimizing the AV trajectory.

5.1 Numerical methods

We briefly describe the implementation of the control law on the AVs to achieve optimal traffic flow using AVs as a moving bottlenecks in the traffic stream. The control of traffic using autonomous vehicles as a moving bottlenecks is implemented as an optimization problem where the maximum speed of each AV is adjusted at an optimal time interval. During each time period, each AV travels at the optimal constant speed, unless it is required to drive slower due to local traffic conditions. For a given initial traffic state (density distribution on the roadway) and starting position of the AVs, the optimal trajectory of each AV is computed that minimizes the total fuel consumption of the entire traffic flow. The optimal trajectory of each AV consists of a series of speeds to drive at for each successive optimal interval, and is based on the predicted traffic state and the corresponding position of each AV as solved using the coupled ODE-PDE system.

More precisely, the N autonomous vehicles adjust their driving speed at the same time and a total of $M-1$ times during the experiment duration. We solve the following approximate optimization problem

$$\inf_{\substack{\{(C_i)_{i\in\{1,\cdots,N\}}/C_i\in[0,V_{\max}]^M\}\\ T\in(0,T_f)^{M-1}}} \mathbf{TFC}(V_1,\cdots,V_N) \qquad (38)$$

where the cost function **TFC** is defined in (18) and, for every $t\in\mathbb{R}_+$,

$$V_i(t)=\sum_{k=1}^{M} C_i(k)\,\mathbb{1}_{(T(k-1),T(k))}(t), \qquad (39)$$

with $T(0):=0$ and $T(N)=+\infty$. The optimization problem (38) is solved using the genetic algorithm as implemented in the Matlab Global Optimization Toolbox (`ga()`). Fixing ρ_0 and $(y_i^0)_{i\in\{1,\cdots,N\}}$, the solution $(\rho,y_1,\cdots,y_N)$ of (1)-(2)-(3) with $(V_i)_{i\in\{1,\cdots,N\}}$ defined in (39) is solved using a wave-front tracking algorithm described in Section 3. Since, in our algorithm, two autonomous vehicles are allowed to interact, leading to a possible interaction between two non-classical shocks, the constraint $y_i(t)-\epsilon<y_{i+1}(t)$ does not appear in (38). Note that each numerical optimal solution $(V_i^{\text{opt}})_{i\in\{1,\cdots,N\}}$ of (38) computed in Section 5 belongs to the class of admissible maximum speed $\mathcal{V}_N^\epsilon$. Thus, the constraint $y_i(t)-\epsilon<y_{i+1}(t)$ is inactive.

5.2 Numerical examples

Using the implementation of the numerical method described in Section 5.1, a numerical example is conducted to demonstrate the ability of AVs to be controlled to act as a moving bottleneck and reduce the fuel consumption of the overall traffic flow. The numerical experiment is conducted over a stretch of highway ($x_1=0$ km and $x_2=50$ km in (18)) over the course of one hour ($T_f=1$ hour in (18)). The maximum speed of each AV on the roadway is $V_{\max}=120$ km/h. The maximum (jam) density on the roadway is considered to be 400 veh/km. Each AV has influence over one of the two lanes ($\alpha=0.6$).

We consider two optimal control approaches for the AV: one in which each AV selects an optimal constant speed for the duration of the experiment, and another in which first one, and the two AVs are allowed to select the optimal speed at up to six distinct points in the simulation. This corresponds to each AV being able to change the driving strategy a total of six times in the one-hour experiment. The results of the numerical experiments are described below.

5.2.1 Optimal constant speeds of multiple AVs over one hour ($M=1$ in (38))

For any constant initial data $\rho_0\in\mathcal{M}_n$, we numerically solve the optimal problem (18) considering three different cases:

(1) When each AV drives at maximum speed $V_{\max}$ over the duration of the numerical experiment, the AVs don't influence the traffic flow.
(2) When only one AV is used, i.e., $N=1$ in (18), we choose $y_1^0=25$ and we denote the approximate optimal solution of (38) as $V_{\text{opt}}^1(\rho_0)$.
(3) When two AVs are used, i.e., $N=2$ in (18), we choose $[y_1^0,y_2^0]=[25,35]$ and we denote the approximate optimal solution of (38) as $(V_1^{\text{opt}}(\rho_0),V_2^{\text{opt}}(\rho_0))$.

The values of $\mathbf{TFC}(V_{\max})$, $\mathbf{TFC}(V_1^{\text{opt}}(\rho_0))$, and $\mathbf{TFC}(V_1^{\text{opt}}(\rho_0),V_2^{\text{opt}}(\rho_0))$ are plotted with respect to the initial data ρ_0 in Figure 4. As shown in the figure, three distinct optimal driving strategies arise:

(1) When the initial density ρ_0 is low ($\rho_0\in(0,87)$ for one AV and $\rho_0\in(0,199)$ for two AVs), the use of a moving bottleneck is needed to optimize (reduce) the total fuel consumption reduce.
(2) When the initial density ρ_0 is moderate ($\rho_0\in(87,326)$ for one AV and $\rho_0\in(199,326)$ for two AVs), the optimal speed of the moving bottleneck is 0 km/h, and thus a fixed bottleneck produces the optimal fuel consumption results when optimizing (18).

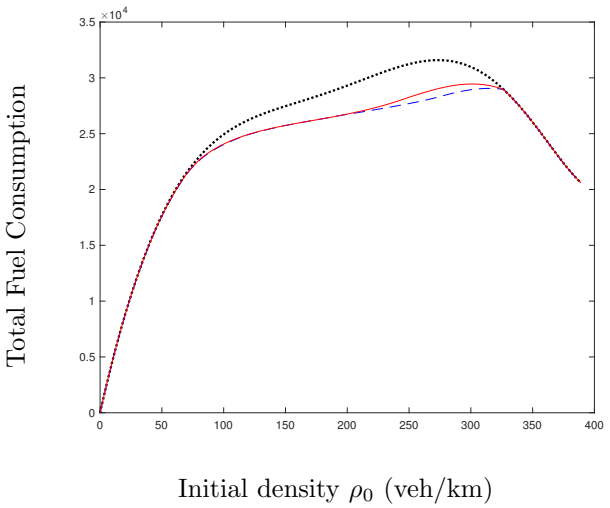

Fig. 4. Plotting of $\mathbf{TFC}(V_{\max})(\cdots)$, $\mathbf{TFC}(V_1^{\text{opt}}(\rho_0))(-)$ and $\mathbf{TFC}(V_1^{\text{opt}}(\rho_0), V_2^{\text{opt}}(\rho_0))(--)$ with respect to the initial data ρ_0.

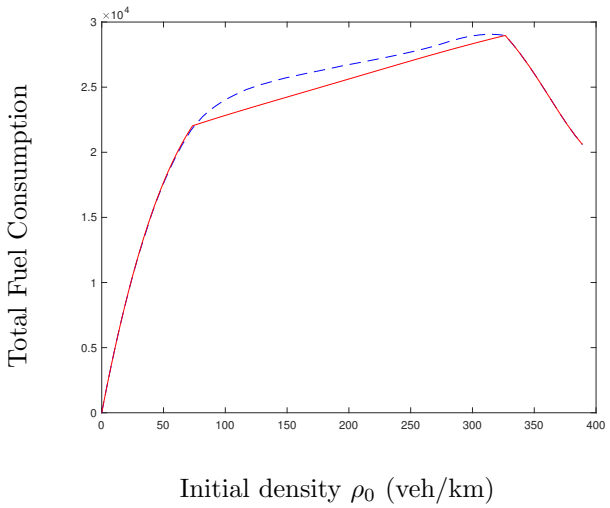

Fig. 5. Plotting of $\mathbf{TFC}(V_1^{\text{opt}}(\rho_0), V_2^{\text{opt}}(\rho_0))(--)$ and $\mathbf{TFC}(0_{11})(-)$ with respect to the initial data ρ_0

(3) When the initial density ρ_0 is high ($\rho_0 \in (326, 400)$ for one and two AVs), the density is too great and the AV is unable to control the traffic flow. Mathematically speaking, the constraint (3) is inactive.

Note that when more AVs are deployed on the road to actively control the flow of traffic and optimize the fuel consumption of the entire fleet, the range of initial densities where a moving bottleneck is needed to optimize the fuel consumption increases.

We consider eleven AVs acting as fixed bottlenecks (i.e., driving with zero speed) starting at $y_i^0 = 5i$ with $i \in \{0, \cdots, 10\}$. We denote the total associated fuel consumption with $\mathbf{TFC}(0_{11})$. The solutions $\mathbf{TFC}(V_1^{\text{opt}}(\rho_0), V_2^{\text{opt}}(\rho_0))$ and $\mathbf{TFC}(0_{11})$ are plotted with respect to the initial data ρ_0 in Figure 5.

5.2.2 *Multiple optimal speeds of multiple AVs over one hour ($M = 6$ in (38))*

In this scenario, the initial traffic state is

$$\rho_0(x) = \begin{cases} 0, & \text{if } x < -35, \\ 121, & \text{if } 35 < x < 0, \\ 80, & \text{if } 0 < x < 50, \\ 371, & \text{if } 50. \end{cases}$$

Moreover, each AV changes its speed six times in the one-hour numerical experiment.

As seen in Figure 6, if the AV drives at the maximum possible velocity at all times, the AV encounters the leading edge of the shock wave after roughly 0.2 hours. This

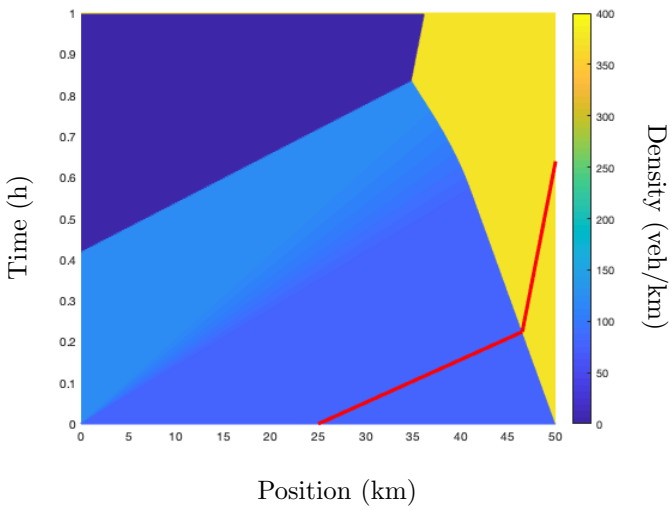

Fig. 6. Traffic density evolution showing wave fronts when the AV, starting at $y_1^0 = 25$, drives at the maximum possible speed at all times. The AV trajectory is plotted in red.

results in a total fuel consumption of 17740 ℓ of fuel. However, when the AV is acting as a moving bottleneck to control the traffic and reduce the fuel consumption, it is able to achieve a lower density gap between the wave and the AV as seen in Figure 7. By using the control strategy optimized with the genetic algorithm, the total fuel consumption for the same traffic flow is reduced to 17613 ℓ, a reduction of 0.72%. When two AV are acting as a moving bottleneck to control the traffic and reduce the fuel consumption, the total fuel consumption for the same traffic flow is reduced to 17487 ℓ, a reduction of 1.43% as seen in Figure 8.

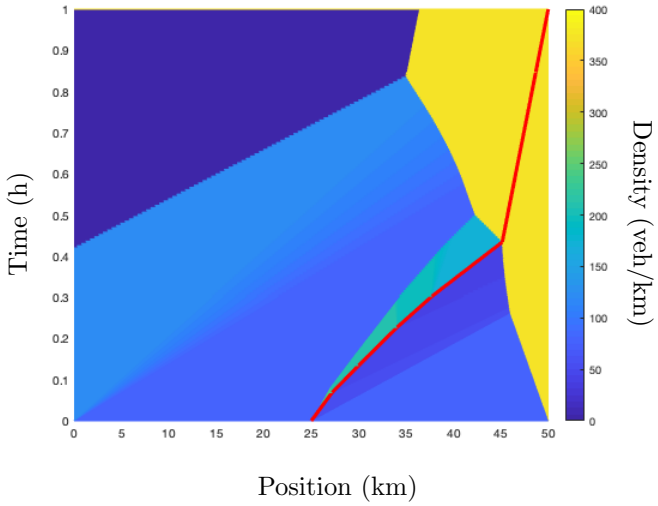

Fig. 7. Traffic density evolution showing wave fronts under the optimal driving strategy with one AV starting at $y_1^0 = 25$. The AV trajectory is plotted in red.

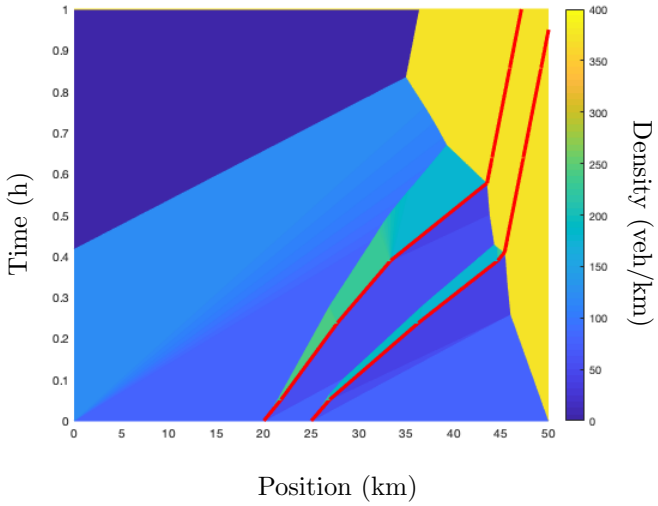

Fig. 8. Traffic density evolution showing wave fronts under the optimal driving strategy with two AVs starting at $[y_0^1, y_0^2] = [20, 25]$. The two AV trajectories are plotted in red.

6 Conclusions

In this work we study a coupled PDE-ODE framework to model the impact of multiple AVs being used as moving bottlenecks to control the flow of traffic and reduce the overall fuel consumption of the entire traffic stream. The main traffic flow is described by a scalar conservation law while the controlled vehicles are described via ODEs. The prove the existence of solutions for the coupled PDE-ODE systems and show how to compute analytically solutions to the Riemann problem and to the Cauchy problem via wave-front tracking approximations. We define an optimal control problem which consists in minimizing the total fuel consumption, using the autonomous vehicles speeds as control variables. We prove that the optimal control problem (18), admits at least one optimal solution. We solve numerically the optimal control problem (18) by using a genetic algorithm. For the numerical solution, the traffic flow and AVs as moving bottlenecks are simulated using wavefront tracking. We find that with more AVs acting as moving bottlenecks, we are able to realize a greater reduction in total fuel consumption when solving the optimal control problem (18). Additionally, with more AVs acting as actuators in the traffic flow, there is a greater region of densities for which a moving bottleneck is able to achieve a greater reduction in total fuel consumption than a fixed bottleneck. i.e., with more AVs actively controlling the traffic flow, the use of moving bottlenecks becomes more efficient. Thus, the findings presented in this paper indicate that it is possible to use a small number of AVs as moving bottlenecks to actively control the flow of traffic and reduce the fuel consumption for the entire vehicle fleet.

7 Acknowledgments

T. Liard was supported by the European Research Council (ERC) under the European Union's Horizon 2020 research and innovation programme (grant agreement No 694126-DYCON).
This work was partially supported by the Inria associated team MEMENTO (Modeling autonomous vehicles in traffic flow.)

References

[1] K. Ahn, H. Rakha, A. Trani, and M. Van Aerde. Estimating vehicle fuel consumption and emissions based on instantaneous speed and acceleration levels. *Journal of transportation engineering*, 128(2):182–190, 2002.

[2] A. Alessandri, A. Di Febbraro, A. Ferrara, and E. Punta. Nonlinear optimization for freeway control using variable-speed signaling. *IEEE Transactions on Vehicular Technology*, 48(6):2042–2052, 1999.

[3] M. K. Banda and M. Herty. Adjoint IMEX-based schemes for control problems governed by hyperbolic conservation laws. *Computational optimization and applications*, 51(2):909–930, 2010.

[4] I. M. Berry. *The effects of driving style and vehicle performance on the real-world fuel consumption of US light-duty vehicles*. PhD thesis, Massachusetts Institute of Technology, 2010.

[5] C. Canudas De Wit. Best-effort highway traffic congestion control via variable speed limits. In *50th IEEE Conference on Decision and Control and European Control Conference*, 2011.

[6] R. C. Carlson, I. Papamichail, M. Papageorgiou, and A. Messmer. Optimal motorway traffic flow control involving variable speed limits and ramp metering. *Transportation Science*, 44:238–253, 2010.

[7] M. Čičić and K. H. Johansson. Traffic regulation via individually controlled automated vehicles: a cell transmission model approach. In *2018 21st International Conference on Intelligent Transportation Systems (ITSC)*, pages 766–771. IEEE, 2018.

[8] A. Csikós, I. Varga, and K. Hangos. Freeway shockwave control using ramp metering and variable speed limits. In *21st Mediterranean Conference on Control & Automation*, pages 1569–1574, 2013.

[9] C. M. Dafermos. Polygonal approximations of solutions of the initial value problem for a conservation law. *Journal of Mathematical Analysis and Applications*, 38:33 – 41, 1972.

[10] C. Daganzo. The cell transmission model: A dynamic representation of highway traffic consistent with the hydrodynamic theory. *Transportation Research Part B*, 28:269–287, 1994.

[11] L. Davis. Effect of adaptive cruise control systems on traffic flow. *Physical Review E*, 69(6):066110, 2004.

[12] M. L. Delle Monache and P. Goatin. Scalar conservation laws with moving constraints arising in traffic flow modeling: an existence result. *Journal of Differential equations*, 257(11):4015–4029, 2014.

[13] J. R. Domíngeuz Frejo and E. F. Camacho. Global versus local MPC algorithms in freeway traffic control with ramp metering and variable speed limits. *IEEE Transactions on intelligent transportation systems*, 13(4):1556–1565, 2012.

[14] L. C. Evans and R. F. Gariepy. *Measure Theory and Fine Properties of Functions*. CRC, 1991.

[15] M. Garavello, P. Goatin, T. Liard, and B. Piccoli. A controlled multiscale model for traffic regulation via autonomous vehicles. *Submitted*, 2019.

[16] M. Guériau, R. Billot, N.-E. El Faouzi, J. Monteil, F. Armetta, and S. Hassas. How to assess the benefits of connected vehicles? a simulation framework for the design of cooperative traffic management strategies. *Transportation research part C: emerging technologies*, 67:266–279, 2016.

[17] A. Hegyi, B. De Schutter, and J. Hellendoorn. Optimal coordination of variable speed limits to suppress shock waves. *IEEE Transactions on Intelligent Transportation Systems*, 6(1):102–112, mar 2005.

[18] Z. Hou, J.-X. Xu, and H. Zhong. Freeway traffic control using iterative learning control-based ramp metering and speed signaling. *IEEE Transactions on vehicular technology*, 56(2):466–477, 2007.

[19] D. Jacquet, M. Krstic, and C. Canudas De Wit. Optimal control of scalar one-dimensional conservation laws. In *Proceedings of the 2006 American Control Conference*, pages 5213–5218, 2006.

[20] I. Karafyllis, N. Bekiaris-Liberis, and M. Papageorgiou. Feedback control of nonlinear hyperbolic pde systems inspired by traffic flow models. *IEEE Transactions on Automatic Control*, 64(9):3647–3662, 2018.

[21] I. Karafyllis and M. Papageorgiou. Feedback control of scalar conservation laws with application to density control in freeways by means of variable speed limits. *Automatica*, 105:228–236, 2019.

[22] F. Knorr, D. Baselt, M. Schreckenberg, and M. Mauve. Reducing traffic jams via vanets. *IEEE Transactions on Vehicular Technology*, 61(8):3490–3498, 2012.

[23] O. Kolb, S. Göttlich, and P. Goatin. Capacity drop and traffic control for a second order traffic model. *Networks and Heterogeneous Media*, 12(4):663–681, oct 2017.

[24] P. D. Lax. Hyperbolic systems of conservation laws ii. *Communications on pure and applied mathematics*, 10(4):537–566, 1957.

[25] J.-P. Lebacque, J. Lesort, and F. Giorgi. Introducing Buses into First-Order Macroscopic Traffic Flow Models. *Transportation Research Record: Journal of the Transportation Research Board*, 1644(98):70–79, jan 1998.

[26] T. Liard and B. Piccoli. On entropic solutions to conservation laws coupled with moving bottlenecks. *Submitted*, 2019.

[27] T. Liard and B. Piccoli. Well-posedness for scalar conservation laws with moving flux constraints. *SIAM Journal on Applied Mathematics*, (2):641–667, 2019.

[28] M. J. Lighthill and G. B. Whitham. On kinematic waves. ii. a theory of traffic flow on long crowded roads. *Proceedings of the Royal Society of London. Series A, Mathematical and Physical Sciences*, 229:317–345, 1955.

[29] G. Piacentini, P. Goatin, and A. Ferrara. Traffic control via moving bottleneck of coordinated vehicles. *IFAC-PapersOnLine*, 51(9):13–18, 2018.

[30] R. A. Ramadan and B. Seibold. Traffic flow control and fuel consumption reduction via moving bottlenecks. *arXiv preprint arXiv:1702.07995*, 2017.

[31] J. Reilly, W. Krichene, M. L. Delle Monache, S. Samaranayake, P. Goatin, and A. M. Bayen. Adjoint-based optimization on a network of discretized scalar conservation law PDEs with applications to coordinated ramp metering. *Journal of optimization theory and applications*, 167(2):733–760, 2015.

[32] P. I. Richards. Shock waves on the highway. *Operations Research*, 4:42–51, 1956.

[33] W. Rudin. *Principles of mathematical analysis*. McGraw-Hill Book Co., New York-Auckland-Düsseldorf, third edition, 1976. International Series in Pure and Applied Mathematics.

[34] I. S. Strub and A. M. Bayen. Weak formulation of boundary conditions for scalar conservation laws: An application to highway traffic modelling. *International Journal of Robust and Nonlinear Control: IFAC-Affiliated Journal*, 16(16):733–748, 2006.

[35] R. E. Stern, S. Cui, M. L. Delle Monache, R. Bhadani, M. Bunting, M. Churchill, N. Hamilton, H. Pohlmann, F. Wu, B. Piccoli, et al. Dissipation of stop-and-go waves via control of autonomous vehicles: Field experiments. *Transportation Research Part C: Emerging Technologies*, 89:205–221, 2018.

[36] A. Talebpour and H. S. Mahmassani. Influence of connected and autonomous vehicles on traffic flow stability and throughput. *Transportation Research Part C: Emerging Technologies*, 71:143–163, 2016.

[37] S. Ulbrich. A sensitivity and adjoint calculus for discontinuous solutions of hyperbolic conservation laws with source terms. *SIAM Journal on control and optimization*, 41(3):740–797, 2002.

[38] S. Ulbrich. Adjoint-based derivative computations for the optimal control of discontinuous solutions of hyperbolic conservations laws. *Systems and control letters*, 48(3):313–328, 2003.

[39] H. Yu and M. Krstic. Traffic congestion control on aw-rascle-zhang model: Full-state feedback. In *2018 Annual American Control Conference (ACC)*, pages 943–948. IEEE, 2018.